Chapter 4

Molecular dissociation of N_2

In this chapter we report the study of multiple ionization and fragmentation of N_2 induced by ion impact. The experimental data were obtained using time and position sensitive detectors in multihit coincidence mode. The details of the experimental setup and data analysis have been described in chapter 2. With $Ar^{q+}(11 \geq q \geq 4)$ at a projectile velocity of 1 atomic unit we observe a total of seven fragmentation channels originating from multiply charged transient molecular ions. The preference of symmetric charge breakup channels over the asymmetric ones is clearly observed. A signature of core excitation of the target followed by Auger emission is observed in the N^{3+} - N^{3+} fragmentation channel. The kinetic energy release spectra of all the observed fragmentation pathways is explained on the basis of calculated *ab initio* potential energy curves reported in chapter 3. The effect of charge state dependence on the KER spectra in the observed fragmentation channels is also discussed.

4.1 Results: N_2 dissociation following Ar^{9+} impact

Figure 4.1 shows the coincidence map of the dissociation of N_2 following Ar^{9+} impact. From the coincidence map, the inter-particle correlations between the different fragment charge states can be clearly identified. Each point in the map is due to the coincident detection of two nitrogen ions originating from the dissociation of N_2^{q+} molecular ion. The dark patches are due to high density of points

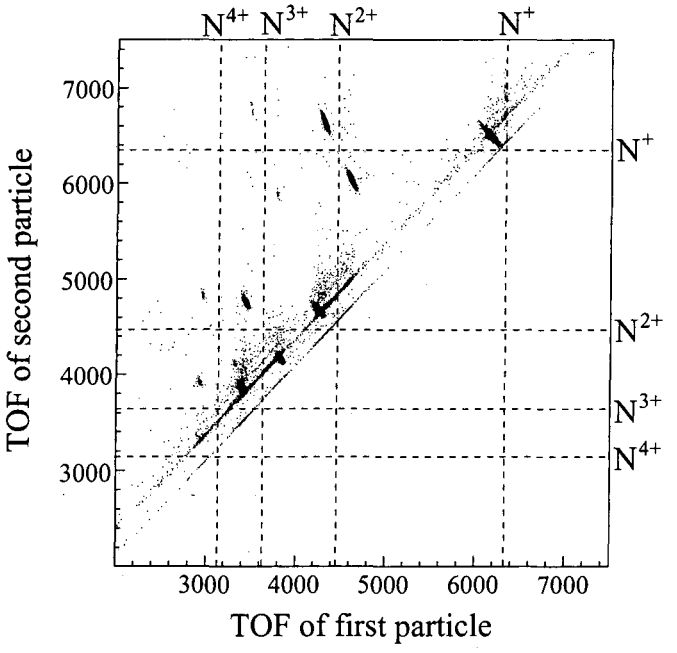

Figure 4.1: Coincidence map of the N_2 fragmentation

representing the various fragmentation pathways. In a majority of the fragmentation channels, the number of counts obtained is reasonably large except for the two fragmentation channels $N^{3+} - N^{1+}$ and $N^{4+} - N^{2+}$ where statistics are low. However, inspite of the low statistics the major energy components of the KER distributions for these channels can be considered since we have eliminated the contributions from the overlap of the N^{3+} forward and N^{4+} backward peaks.

Figures 4.2 to 4.6 show the KER distributions for the dissociation channels observed in this experiment. Almost all the KER spectra obtained in the present experiment exhibit a high energy tail beyond the peak of the KER distribution. Table 4.1 lists the most probable KER values for the different fragmentation channels obtained in the present experiment along with the KER values from other experiments studying N_2 fragmentation. The values calculated from pure Coulomb explosion model (see discussion) are also listed.

Table 4.1: This table shows the KER values obtained for the various fragmentation channels N^{r+} - N^{s+} in N_2 fragmentation induced by ion impact. The values calculated from pure Coulomb explosion model are also included.

Fragmentation Channel	KER values (eV) for different velocities 5.9 MeV/amu [1]	0.2 keV/amu [2]	24 keV/amu (this work)	Coulomb energies (eV) R_e=1.089Å
N^{1+} - N^{1+}	14.5	10.6	7.5, 14.5	13.1
N^{1+} - N^{2+}	30.3	22.2	20	26.2
N^{1+} - N^{3+}	53.5		20, 44	39.3
N^{2+} - N^{2+}	51.3	39.0	32.5	52.5
N^{2+} - N^{3+}	79.9	72.2	68	78.7
N^{2+} - N^{4+}	103.2		40, 100	104.9
N^{3+} - N^{3+}	108.7	112.6	72, 105	118.0

It is to be noted that for N_2^{q+} molecular ion dissociating into $N^{m+} - N^{n+}$, the ones with even q we observe dissociations with m=n, the symmetric charge breakup channel and also m=n+2, the asymmetric charge breakup channel. In case of odd q-values we observe channels with m=n+1 only.

To investigate the peaks of the KER spectra, we have calculated *ab initio* potential energy curves for some of the low lying states of N_2^{q+} ($3 \leq q \leq 6$) molecular ions. The details of these calculations are presented in chapter 3. Table 4.2 shows the results of our calculations in terms of KERs when the various states of the N_2^{q+} ($3 \leq q \leq 6$) molecular ion decays into two atomic fragments in their lowest possible states. Thus the tabulated values of the KER denotes the upper limit of the KER in each fragmentation channel. We now discuss each of the fragmentation channel individually.

4.1.1 Decay of N_2^{2+}

The KER spectrum corresponding to $N^+ - N^+$ fragmentation channel (figure 4.2) shows two major energy components, one at 7.5 eV and another at 14.5 eV. Table 4.3 lists the various molecular states of N_2^{2+} (taken from [4]) and the associated energy release, when they dissociate into two N^+ ions in their ^3P ground

Table 4.2: Theoretically calculated values of KER in case of N_2^{q+} ($3 \leq q \leq 6$) dissociating to the lowest possible states of N^{m+} + N^{n+} with m+n=q. These values denote the upper limit of the KER.

Dissociation channels	Kinetic energy release (eV)
$N_2^{3+}\ ^2\Sigma \rightarrow N^{2+}(^2P) + N^{1+}(^3P)$	25.40
$N_2^{3+}\ ^4\Sigma \rightarrow N^{2+}(^2P) + N^{1+}(^3P)$	19.77
$N_2^{4+}\ a^5\Sigma \rightarrow N^{2+}(^2P) + N^{2+}(^4P)$	35.48
$N_2^{4+}\ a^5\Sigma \rightarrow N^{1+}(^3P) + N^{3+}(^3P)$	33.07
$N_2^{4+}\ b^5\Sigma \rightarrow N^{2+}(^2P) + N^{2+}(^4P)$	45.40
$N_2^{4+}\ b^5\Sigma \rightarrow N^{1+}(^3P) + N^{3+}(^3P)$	42.89
$N_2^{4+}\ ^3\Sigma \rightarrow N^{2+}(^2P) + N^{2+}(^2P)$	46.59
$N_2^{4+}\ ^3\Sigma \rightarrow N^{1+}(^3P) + N^{3+}(^1S)$	28.78
$N_2^{5+}\ ^2\Sigma \rightarrow N^{2+}(^2P) + N^{3+}(^1S)$	67.56
$N_2^{5+}\ ^4\Sigma \rightarrow N^{2+}(^4P) + N^{3+}(^1S)$	59.68
$N_2^{6+}\ ^1\Sigma \rightarrow N^{3+}(^1S) + N^{3+}(^1S)$	114.67
$N_2^{6+}\ ^1\Sigma \rightarrow N^{2+}(^2P) + N^{4+}(^2S)$	86.96
$N_2^{6+}\ ^3\Sigma \rightarrow N^{3+}(^1S) + N^{3+}(^3P)$	98.46
$N_2^{6+}\ ^3\Sigma \rightarrow N^{2+}(^4P) + N^{4+}(^2S)$	69.80

state. Many of these states are metastable in their lowest vibrational levels with very long tunneling lifetimes. In the present experiment, only the higher vibrational levels of these states are excited by a vertical Frank Condon transition and undergo dissociation releasing energy. The theoretical energy release values are in good agreement with the experimentally obtained KER values. In electron impact ionization experiments [5] similar energy releases have been observed for N_2^{2+} decay. The higher resolution in those experiments enable the separation of the individual vibrational levels leading to dissociation into $N^+ - N^+$ ion pair. In the present experiment excitation into the low lying $a^3\Pi_u$ and $A^1\Pi_u$ states of N_2^{2+} have not being observed.

4.1.2 Decay of N_2^{3+}

The maximum KER that can be released on dissociation of N_2^{3+} is 25.40eV. The peak of the KER spectra of the $N^+ - N^{2+}$ fragmentation channel (figure 4.3)

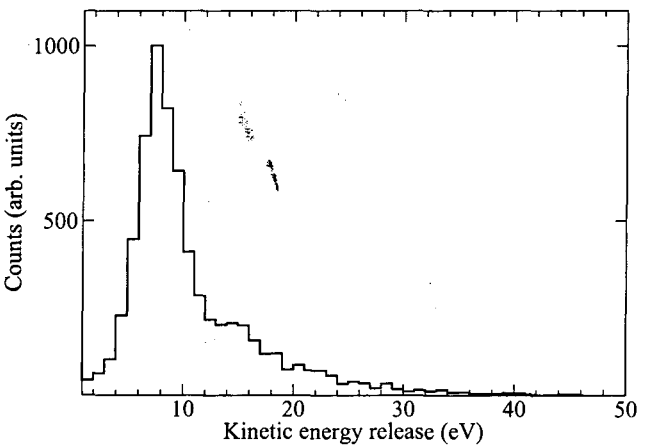

Figure 4.2: Kinetic energy release spectra of the $N^+ - N^+$ fragmentation channel

Table 4.3: The possible molecular states of N_2^{2+} dissociating into $N^+(^3P) + N^+(^3P)$ along with the theoretically calculated values of KER taken from reference [4]

Molecular states	Release energy(eV)
$d^1\Sigma_g^+$	8.4
$c^1\Delta_g$	8.1
$D^3\Pi_g$	7.9
$g^1\Sigma_g^+$	14.2
$h^1\Sigma_u^-$	14.9
$G^3\Pi_g$	15.2
$B^3\Sigma_u^-$	14.1

occurs at around 20 eV and can be explained by considering the decay of N_2^{3+} to N^{2+} (^{2}P), the ground state of N^{2+} and N^{1+} (^{1}S), the excited state of N^{1+}.

$$N_2^{3+}\ ^2\Sigma \rightarrow N^{2+}(^2P) + N^{1+}(^1S),\quad 21.35eV$$

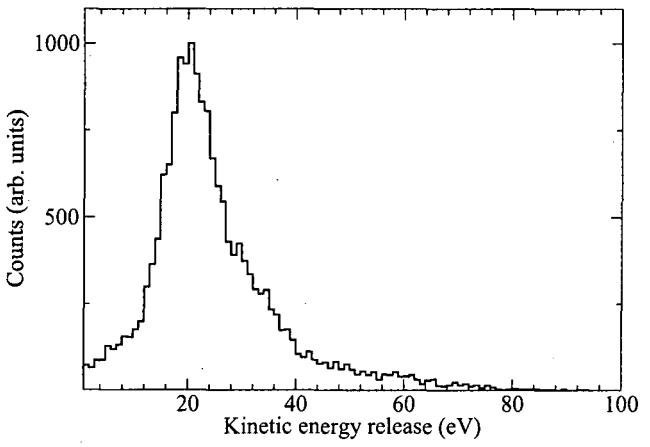

Figure 4.3: Kinetic energy release spectra of the $N^+ - N^{2+}$ fragmentation channel

Table 4.4: Results of theoretical calculations for N_2^{3+} dissociation taken from reference [6]

Fragmentation Channel	Release energy(eV)
$N_2^{3+}(^2\Pi_g) \rightarrow N^{2+}(^2P) + N^{1+}(^3P)$	16.6
$N_2^{3+}(^2\Sigma_g) \rightarrow N^{2+}(^2P) + N^{1+}(^3P)$	17.1
$N_2^{3+}(^4\Pi_u) \rightarrow N^{2+}(^2P) + N^{1+}(^3P)$	23.4
$N_2^{3+}(^4\Sigma_g) \rightarrow N^{2+}(^2P) + N^{1+}(^3P)$	23.9
$N_2^{3+}(^4\Sigma_u) \rightarrow N^{2+}(^2P) + N^{1+}(^3P)$	26.4

The high energy components of the KER spectra are possibly coming from the dissociation of the higher excited states of N_2^{3+}. Our values for the lowest electronic state of the N_2^{3+} molecular ion are in agreement with the calculations given in reference [6] and the high energy component of our KER spectra can be explained on the basis of the higher excited states of N_2^{3+} calculated in the same reference. Some of the results of reference [6] are tabulated in 4.4 for comparison.

4.1.3 Decay of N_2^{4+}

The N_2^{4+} molecular ion can dissociate to give either $N^{2+} - N^{2+}$ (the symmetric channel) or $N^{+} - N^{3+}$ (the asymmetric channel) (figure 4.4). The dominant channel observed is the symmetric one. Our calculations for the lowest states of N_2^{4+} explains the KER spectrum of the $N^{2+} - N^{2+}$ and $N^{+} - N^{3+}$ fragmentation channels. In cases where the KER value is lower than the maximum KER (Table 4.2) the decay to excited states of the atomic fragments explains the experimentally observed values.

$$
\begin{aligned}
N_2^{4+} b\,^5\Sigma &\rightarrow N^{2+}(^2D) + N^{2+}(^4P) \quad , 32.88eV \\
N_2^{4+} a\,^5\Sigma &\rightarrow N^{1+}(^3D) + N^{3+}(^3P) \quad , 21.64eV \\
N_2^{4+} b\,^5\Sigma &\rightarrow N^{1+}(^3P) + N^{3+}(^3P) \quad , 42.89eV
\end{aligned}
$$

In the Frank Condon region the $a^5\Sigma$ state is the ground state of the N_2^{4+} molecular ion. It cannot dissociate into two N^{2+} ions in their ^{2}P ground states because of the spin conservation rules. It can however decay into one ground state $N^{2+}(^2P)$ and one excited $N^{2+}(^4P)$ ion with the release of 35.48 eV as KER. The most probable energy of 32.5 eV obtained in our experiment is lower than this by about 5 eV which can result if $b^5\Sigma$ decays into two excited states of N^{2+}, the (^4P) and the (^2D) state.

The KER spectra for the $N^{+} - N^{3+}$ channel shows two energy components. The lower energy component around 20 eV can come from the decay of $a^5\Sigma$ into $N^{1+}(^3D) + N^{3+}(^3P)$ releasing around 21.64 eV. The origin of the high energy component (44 eV) is the decay of $b^5\Sigma$ into $N^{1+}(^3P) + N^{3+}(^3P)$ releasing around 42.89 eV energy.

4.1.4 Decay of N_2^{5+}

The fragmentation channel of $N^{2+} - N^{3+}$ (figure 4.5) has its origin in the dissociation of the N_2^{5+} molecular ion. The most probable KER value in this case is around 68 eV. From our calculated potential energy curve for N_2^{5+} we find that the dissociation of the $^2\Sigma$ ground state of this ion into two ground state ions of

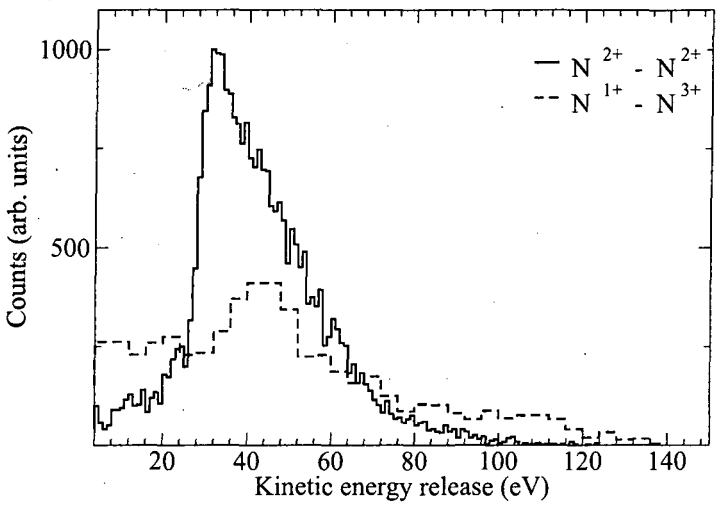

Figure 4.4: Kinetic energy release spectra of the $N^{2+} - N^{2+}$ and $N^{1+} - N^{3+}$ fragmentation channel

$N^{2+}(^2P)$ and $N^{3+}(^1S)$ explains the most probable KER.

$$N_2^{5+}\ ^2\Sigma \rightarrow N^{2+}(^2P) + N^{3+}(^1S) \quad , 67.56eV$$

4.1.5 Decay of N_2^{6+}

In this case, as for the N_2^{4+}, we find that the symmetric channel dominates the fragmentation products. The high energy peak in the KER spectra of $N^{3+} - N^{3+}$ channel (figure 4.6) at around 105 eV can be explained from our UHF calculations on N_2^{6+} molecular ion.

$$N_2^{6+}\ ^1\Sigma \rightarrow N^{3+}(^1S) + N^{3+}(^1S) \quad , 114.7eV$$

Our UHF calculations are in reasonable agreement with the experimentally obtained value. Although we cannot identify the most probable KER value for the $N^{2+} - N^{4+}$ fragmentation channel due to poor statistics, two distinct energy com-

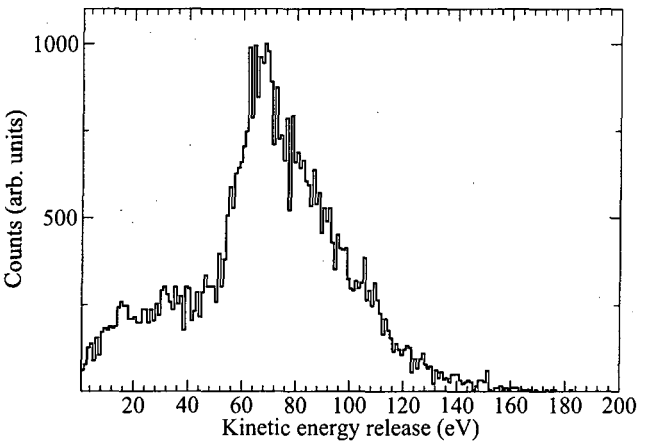

Figure 4.5: Kinetic energy release spectra of the $N^{2+} - N^{3+}$ fragmentation channel

ponents are clearly visible in the KER spectrum. The low energy component (40 eV) in this channel can be explained from the decay of the transient $^3\Sigma$ state of the molecular N_2^{6+} ion decaying into ground as well as excited states of the atomic fragments. The high energy component above 100 eV cannot be explained from the low lying $^1\Sigma$ and $^3\Sigma$ states of N_2^{6+}. This component is possibly coming from the higher excited states of the N_2^{6+} molecular ion.

$$
\begin{aligned}
N_2^{6+}\,{}^3\Sigma &\rightarrow N^{2+}(^2P) + N^{4+}(^2S) \quad , 86.96eV \\
N_2^{6+}\,{}^3\Sigma &\rightarrow N^{2+}(^4P) + N^{4+}(^2S) \quad , 69.8eV \\
N_2^{6+}\,{}^3\Sigma &\rightarrow N^{2+}(^2P) + N^{4+}(^4P) \quad , 35.4eV \\
N_2^{6+}\,{}^3\Sigma &\rightarrow N^{2+}(^4P) + N^{4+}(^4P) \quad , 28.3eV \\
N_2^{6+}\,{}^3\Sigma &\rightarrow N^{2+}(^2D) + N^{4+}(^4P) \quad , 22.9eV
\end{aligned}
$$

The low energy sharp peak at around 72 eV in the $N^{3+} - N^{3+}$ fragmentation channel cannot be explained by molecular dissociation of N_2^{6+}. This energy is the very close to the most probable KER in case of N_2^{5+} fragmentation (68 eV). The difference of around 4 eV in the most probable KER obtained in case of $N^{2+} - N^{3+}$ fragmentation channel and the low energy peak in the $N^{3+} - N^{3+}$ KER

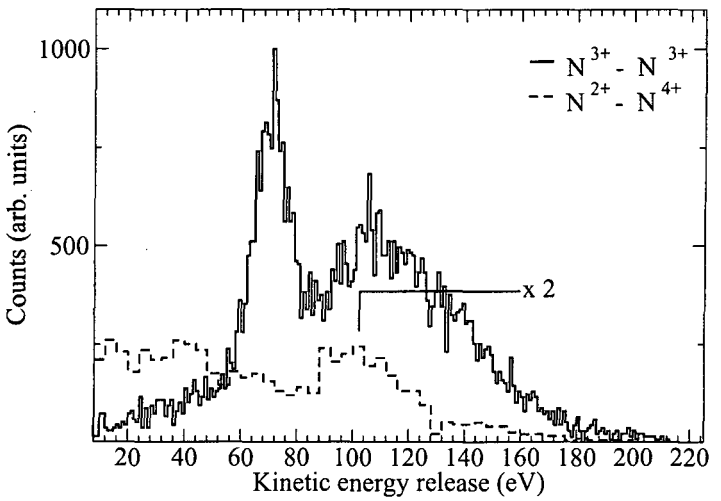

Figure 4.6: Kinetic energy release spectra of the $N^{3+} - N^{3+}$ and $N^{2+} - N^{4+}$ fragmentation channel

spectra can be explained by the population of highly excited states of N_2^{5+} transient molecular ion dissociating into $N^{2+} - N^{3+}$. The origin of this energy component thus lies in the Auger decay of the N^{2+} ion formed from the dissociation of highly excited states of N_2^{5+} into N^{2+} and N^{3+}.

4.2 Charge state dependence of KERD

Figures 4.7 to 4.13 show the KER distributions for the dissociation channels observed in this experiment as a function of the incident projectile charge. The projectile velocity was kept constant at 1 a.u. so that there is no change in the ion-molecule interaction time. No additional energy component is observed in any of the fragmentation channel on varying the projectile charge. Except for the $N^{3+} - N^{3+}$ fragmentation channel in which we observe a major difference in the relative intensities of the two peaks, all the other fragmentation channels show similar KER distributions even on varying the projectile charge. Only small differences in intensities and energy spans can be seen.

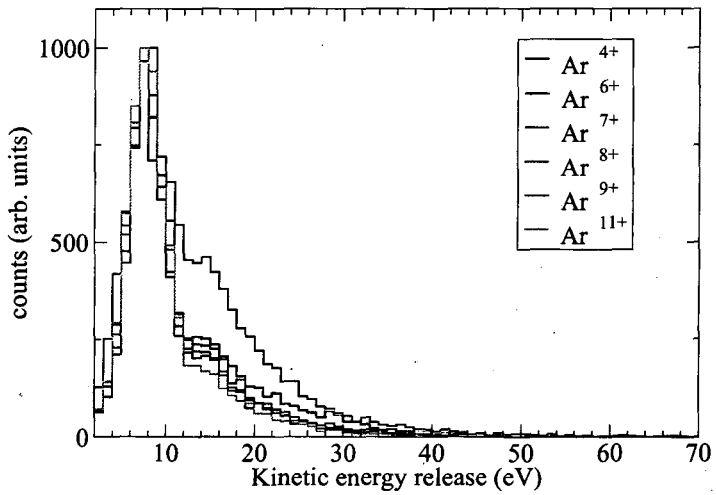

Figure 4.7: Kinetic energy release spectra of the $N^{1+} - N^{1+}$ fragmentation channel obtained for different incident projectile charge state.

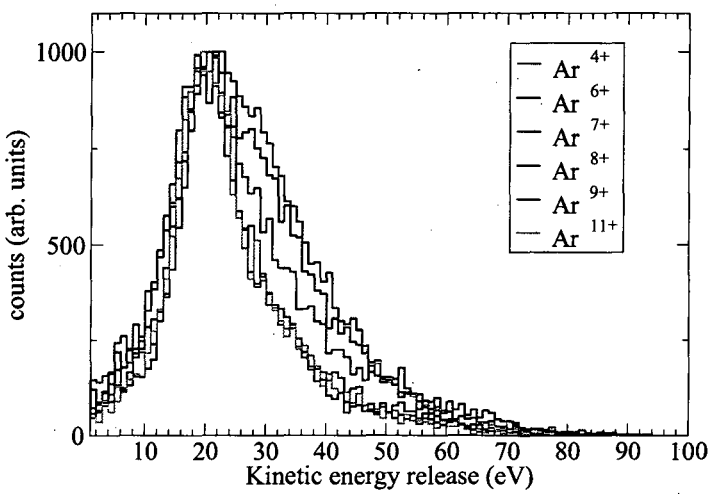

Figure 4.8: Kinetic energy release spectra of the $N^{1+} - N^{2+}$ fragmentation channel obtained for different incident projectile charge state.

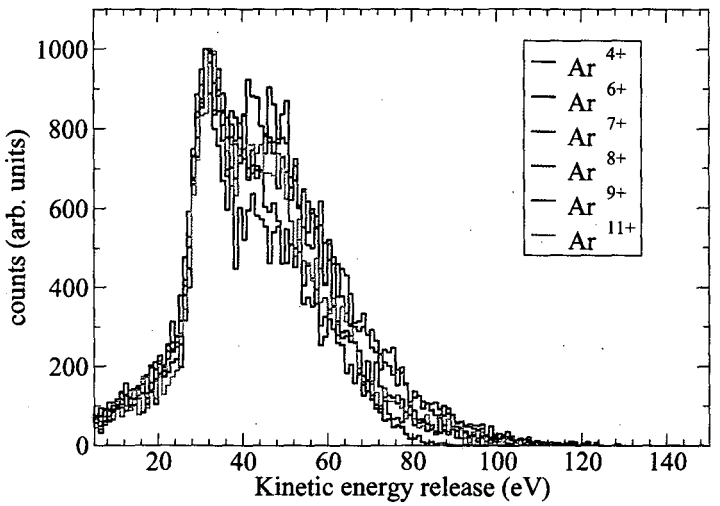

Figure 4.9: Kinetic energy release spectra of the $N^{2+} - N^{2+}$ fragmentation channel obtained for different incident projectile charge state.

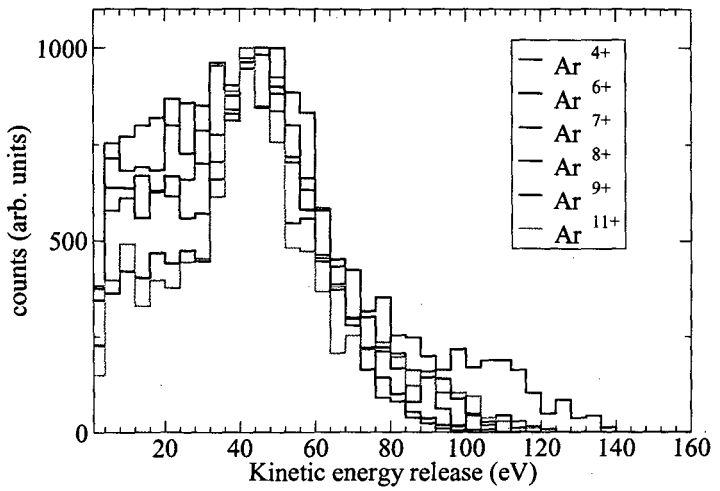

Figure 4.10: Kinetic energy release spectra of the $N^{1+} - N^{3+}$ fragmentation channel obtained for different incident projectile charge state.

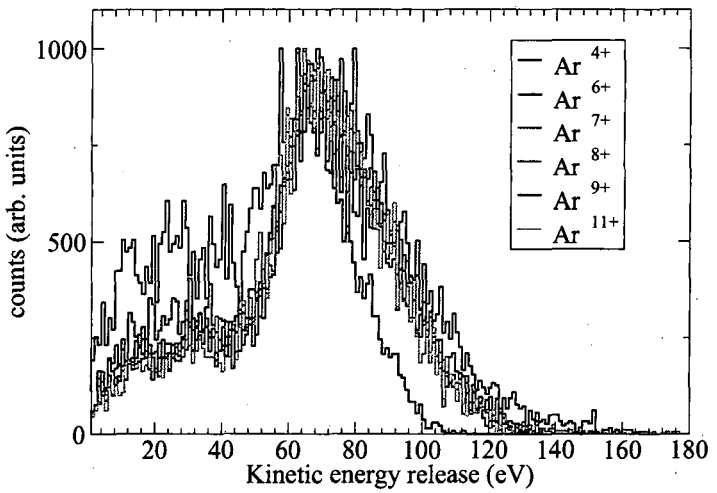

Figure 4.11: Kinetic energy release spectra of the $N^{2+} - N^{3+}$ fragmentation channel obtained for different incident projectile charge state.

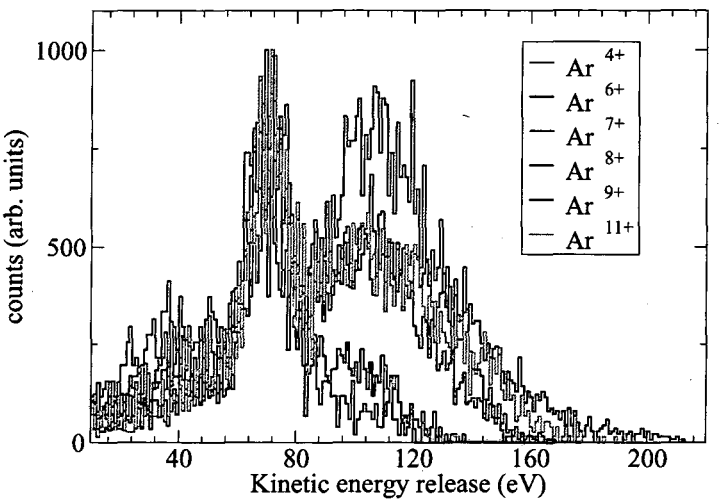

Figure 4.12: Kinetic energy release spectra of the $N^{3+} - N^{3+}$ fragmentation channel obtained for different incident projectile charge state.

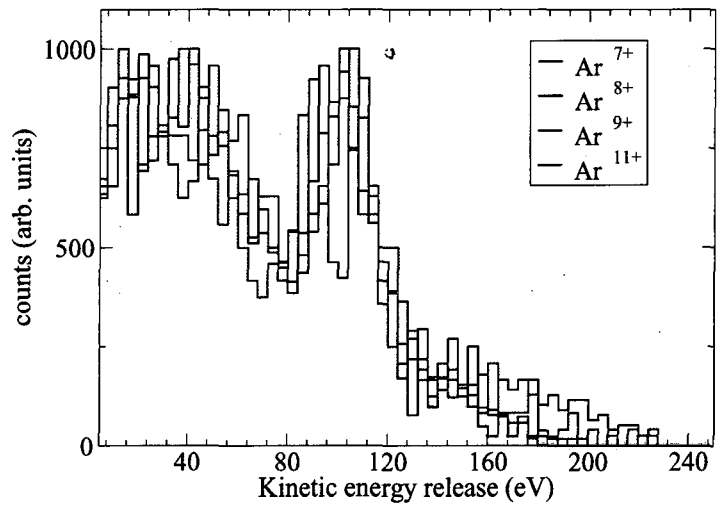

Figure 4.13: Kinetic energy release spectra of the $N^{2+} - N^{4+}$ fragmentation channel obtained for different incident projectile charge state.

The following two competing processes are responsible for the production of the $N^{3+} - N^{3+}$ fragment pair

- The dissociation of N_2^{5+} resulting in the $N^{2+} - N^{3+}$ fragment pair and the subsequent Auger relaxation of the N^{2+} fragment to give N^{3+}. This is an indirect process resulting in an energy distribution whose most probable value is at 72eV.

- The dissociation of N_2^{6+} transient molecular ion resulting in the $N^{3+} - N^{3+}$ fragment pair. This is a direct process, the most probable KER for which is around 105eV.

From figure 4.12 we note that for the $N^{3+} - N^{3+}$ fragmentation channel the intensities of two peaks are almost equal in case of fragmentation induced by Ar^{8+}. For both higher and lower projectile charge states (Ar^{7+},Ar^{9+},Ar^{11+}) there is a reduction in the intensity of the the peak originating from the direct process as compared to the intensity from the indirect process. There is very little contribution of the direct process in case of fragmentation induced by Ar^{4+} and Ar^{6+} projectiles as the cross section for the removal of six electrons from N_2 by these two projectiles would be obviously low.

4.3 Discussion

Experimental measurements of the KER's have shown that the energy releases are usually lower than those predicted by the Coulomb explosion model (E (eV)=14.4q_1q_2/R (Å), where q_1 and q_2 is the charge on the two fragments and R is the internuclear distance of the neutral parent molecule).In the Coulomb explosion model, the simplest model describing breakup of molecular ions, a point charge is put on each atom of a molecular ion and the motion of each atom is governed by the Coulomb repulsion from the others.Since the Coulomb explosion model doesn't take into account the electronic charge cloud in the internuclear region generally it predicts a higher KER than that obtained experimentally. In a simple Coulombic model the width of the KER distribution is determined by the

reflection of the ground state probability density off the Coulomb potential curve [8]. The resulting KER distribution is approximately a Gaussian with a width of a few eV [9, 10] which is much less than the observed width of upto 120-140 eV for higher degrees of ionization in the present experiment. Hence the Coulomb explosion model is insufficient to explain either the most probable KER or the observed width of the KER spectra.

In case the fragmented atomic ions are left in an excited state upon molecular dissociation the resultant KER would be lower than that expected with the fragment ions in their respective ground states. On the other hand excited transient molecular ions dissociating into ground state atomic fragments would result in a higher KER as compared to that obtained on dissociation of ground state molecular ions. The high energy component observed in almost all the KER spectra thus hints towards the contribution of excited molecular states to the KER spectra.

Experiments studying N_2 dissociation at high impact energies [1] have yielded higher values of KER than those obtained in the present experiment. This is possibly because at high projectile energies, higher excited states of N_2^{q+} molecular ions are populated leading to larger KER values on dissociation.

Remscheid *et al* [2] have calculated potential energy curves for N_2^{4+} and N_2^{6+} molecular ions to explain their study on N_2 fragmentation induced by Ar^{8+} (8 keV) projectile. They have concentrated on the symmetric channel of charge breakup of N_2^{4+} and N_2^{6+}. In our experiment we observe both the symmetric and the asymmetric charge breakup of the N_2^{4+} and N_2^{6+}. We have calculated the potential energy curves for these molecular ions to investigate the origin of the energy peaks in our KER spectra. For the symmetric breakup, our theoretical values are in agreement with those obtained by Remscheid *et al.* They have calculated two lowest electronic states of the N_2^{4+} transient molecular ion, the $^5\Sigma_u^+$ ground state and the $^3\Sigma_g^-$ state. Although the major component in the KER spectra of $N^{2+} - N^{2+}$ obtained in our experiment comes from the dissociation of the $^5\Sigma$ ground state of N_2^{4+} into $N^{2+}(^4P)$ and $N^{2+}(^2D)$ but there is also a high energy component part of which could be the contribution from the $^3\Sigma$ state of N_2^{4+} dissociating into two ground state $N^{2+}(^2P)$. The dissociation energy for N_2^{6+} as calculated by Remscheid *et al* agree with our experimental as well as our theoretically calculated values.

From the comparative yield of the two ion pairs which correspond to different dissociation channels of a single parent molecular ion we find that the symmetric breakup is preferred over asymmetric, in agreement with the experimental observations of reference [2]. From the comparisons of the KER distributions of such ion pairs we observe that for the asymmetric charge dissociation channel there are two energy components in the KER distribution while the charge symmetric channel has a single peak for the most probable KER. Also in case of N_2^{4+} and N_2^{6+} breakup the two possible channels (symmetric breakup and asymmetric breakup) show different energy components. This implies that the states leading to the symmetric and the asymmetric breakup are independent of each other. This is in contrast to the case for high energy collisions where the KER distributions are very similar for different dissociation channels of the same parent molecular ion indicating a strong inter-channel interaction during dissociation [1].

At the projectile velocity range used in the present experiment, transfer ionisation is the dominant process of electron transfer [7] and thus there is a possibility of the target being left in an excited state after the ion-molecule interaction. The excited particle then relaxes to the ground state either by Auger emission or by radiative decay. The Auger emission lifetimes are of the same order as the characteristic fragmentation time of the molecules and hence only an energy analysis of the emitted electrons in case of ion-molecule collisions can explain the origin of the emitted electrons. Target excitation following ion impact has been observed to play a significant role in multi-electron capture studies in ion-atom collision experiments [11]. Not many reports exist to comment on the role of target excitation in ion-molecule collisions. Lablanquie *et al* [12] had reported the possibility of autoionization in CO^+ leading to production of C^+ and O^+ ions with low kinetic energy releases. A later study [13] using high and low energy projectiles interacting with CO has however indicated that target excitation does not seem to take place. The occurrence of a low energy peak at 72 eV in the $N^{3+} - N^{3+}$ fragmentation channel is a strong evidence of core excitation of N_2 during ion impact as this peak can only be explained by the Auger emission of N^{2+} formed during the dissociation of N_2^{5+} into N^{2+} and N^{3+}. It is worth noting that the relative cross section for production of $N^{3+} - N^{3+}$ ion pair following Auger emission is much greater than its production following decay of N_2^{6+} transient molecular ion. This

implies that the probability of direct ionization of six electrons is less than the probabilty of five electron ionization accompanied by core excitation.

4.4 Conclusion

We have presented the results of a study of ion induced fragmentation of N_2 using time of flight coincidence techniques. The time and position data obtained during the experiment was analysed on event-by-event basis to determine the KER spectra corresponding to the various observed fragmentation channels. The KER spectra is explained on the basis of existing and calculated *ab initio* potential energy curves of the molecular N_2^{q+} ions with ($3 \leq q \leq 6$). Good agreement is found between the theoretically calculated and experimentally determined KER values. The high energy component in almost all the KER spectra originates from the population of the excited intermediate molecular states resulting in the formation of low lying atomic fragments. We have found a signature of core excitation of the target molecule following ion impact in the form of a clear distinct peak at 72 eV in the $N^{3+} - N^{3+}$ KER spectra having an energy close to the probable KER in case of $N^{2+} - N^{3+}$ fragmentation channel. The origin of this peak lies in the Auger emission of the N^{2+} ion formed during the dissociation of N_2^{5+} transient molecular ion into N^{2+} and N^{3+}. Further studies measuring the energy of the emitted electrons are needed to verify the origin of the electrons and identify the role of target excitation in ion-molecule collisions.

Bibliography

[1] B. Siegmann, U. Werner, R. Mann, N. M. Kabachnik, and H. O. Lutz, Phys. Rev. A **62**, 022718 (2000).

[2] A. Remscheid, B. A. Huber, M. Pykavyj, V. Staemmler, and K. Wiesemann, J. Phys. B **29**, 515 (1996).

[3] M.W.Schmidt and *et al.* J. Comput. Chem. **14**, 1347 (1993).

[4] R. W. Wetmore and R. K. Boyd J. Phys. Chem. **90**, 5540 (1986).

[5] M. Lundqvist, D. Edvardsson, P. Baltzer and B. Wannberg, J. Phys. B **29**, 1489 (1996).

[6] A. D. Bandrauk, D. G Musaev, and K. Morokuma, Phys. Rev. A **59**, 4309 (1999).

[7] W. Groh, A. Muller, A. S. Schlachter, and E. Salzborn, J. Phys. B **16**, 1997 (1983).

[8] C. J. Latimer Adv. At. Mol. Opt. Phys. **30**, 105 (1993).

[9] I. Ben-Itzhak, S. G. Ginther,V. Krishnamurthi, and K. D. Carnes, Phys. Rev. A **51**, 391 (1995).

[10] U. Brikmann, A. Reinkoster, B. Siegmann, U. Werner, H. O. Lutz and R. Mann, Physica Scripta **51**, 171 (1999).

[11] A. A. Hasan, E. D. Emmons, G. Hinojosa, and R. Ali, Phys. Rev. Lett. **83**, 4522 (1999).

[12] P. Lablanquie, J. Delwiche, M. -J. Hubin-Franskin, I. Nenner, P. Morin, K. Ito, J. H. D. Eland, J. -M. Robbe, G. Gandara, J. Fournier, and P. G. Fournier, Phys. Rev. A **40**, 5673 (1989).

[13] M. Tarisien, L. Adoui, F. Frémont, D. Leliévre, L. Guillaume, J-Y Chesnel, H. Zhang, A. Dubois, D. Mathur, Sanjay Kumar, M. Krishnamurthy, and A. Cassimi, J. Phys. B **33**, L11 (2000).